

# Imaging structural details in closely related molecular adsorbate systems

V.M. Hallmark and S. Chiang

*IBM Research Division, Almaden Research Center, 650 Harry Road, San Jose, CA 95120-6099, USA*

Received 2 November 1992; accepted for publication 28 December 1992

Monolayer and submonolayer coverages of naphthalene, azulene and methylazulene adsorbed onto Pt(111) have been imaged with molecular resolution. Comparisons of the adsorbate images of azulene with those obtained from its isomer, naphthalene, reveal that binding for the two closely related species is quite different. Naphthalene occupies an adsorption site on the Pt(111) surface with three equivalent orientational minima, while azulene exhibits no clear orientation with the metal substrate lattice. At less than saturation coverage, naphthalene undergoes discrete rotation among the three allowed orientations and translation between adjacent binding sites on a time scale of minutes, but azulene diffusion rates at room temperature are approximately two orders of magnitude faster. Substitution of a single methyl group onto azulene slows the molecular diffusion to an intermediate rate and enables imaging of the distinct adsorbate asymmetry for two methylazulene isomers. Coadsorbing naphthalene with azulene or methylazulene allows direct comparison of localization characteristics as well as internal structure and orientation.

## 1. Introduction

Scanning tunneling microscopy (STM) is emerging as an invaluable tool for obtaining real space images of metal and semiconductor surfaces and adsorbate systems. Although many STM investigations of molecular adsorbates in air have been reported, STM imaging in air severely restricts the choice of substrate and does not provide the standards of characterization and control typical of ultrahigh vacuum (UHV) surface science preparation and analysis techniques. STM studies of molecular systems in UHV to date have been limited to only a few systems, including benzene and carbon monoxide coadsorbed on Rh(111) [1–3], copper phthalocyanine adsorbed onto Cu(111) [4], and naphthalene on Pt(111) [5–7]. These systems produced ultrahigh resolution images of molecular adsorbates as well as varying degrees of detail about adsorption sites, orientation and packing.

These studies demonstrate the power of STM for exploring molecular adsorbate systems, and illustrate the new level of understanding of molecular adsorption to be gained with real space

imaging. But much of the ultimate utility of STM for observing molecular adsorbates lies in its potential to analyze structure in complex, unknown systems or to monitor surface reactions on a molecular scale. For these applications, real-space imaging with submolecular resolution will be required not only to recognize individual molecules of a single species, but to discern subtle differences in adsorbate structure, binding and orientation. To this end, the work presented herein describes an initial study of the capabilities of the STM to distinguish among a series of closely related molecular adsorbates. The selected molecular series includes the previously studied adsorbate naphthalene [5–7] along with its isomer azulene and several novel substituted azulenes, with the various molecules imaged both as pure and coadsorbed overlayers on Pt(111).

## 2. Experimental

All measurements were performed in a multi-chamber, ultrahigh vacuum system with base pressure  $< 10^{-10}$  Torr. The Pt(111) sample was

cleaned by pretreatment in  $10^{-6}$  Torr oxygen at  $650^{\circ}\text{C}$  to remove bulk carbon. Routine cleaning entailed repeated cycles of 500 V  $\text{Ar}^+$  sputtering and annealing between  $800$  and  $900^{\circ}\text{C}$ . Residual carbon contamination was typically below Auger electron spectroscopy detection levels, although surface carbon concentrations as measured by STM were quite variable and locally could approach 4%. Azulene and naphthalene from Aldrich and methylazulene (60% 1-methylazulene and 30% 2-methylazulene) from Sigma were used as received, after degassing by alternately freezing and melting under vacuum. Exposures of the Pt(111) surface to the molecules were made by backfilling the preparation chamber to  $5 \times 10^{-9}$  Torr from a gas manifold maintained at  $75^{\circ}\text{C}$  for naphthalene and azulene, and at  $50^{\circ}\text{C}$  for methylazulene. Ordered monolayers were prepared by exposure with the Pt(111) sample at elevated temperature ( $100$  to  $200^{\circ}\text{C}$ ). This temperature measurement was of limited accuracy because the sample is movable throughout the vacuum system. However, the known decomposition of both azulene and naphthalene near  $200^{\circ}\text{C}$  provided an upper bound for the substrate temperature, while the temperature minimum was judged by the successful acquisition of the ordered ( $6 \times 3$ ) LEED pattern for naphthalene on Pt(111). Mixed monolayers were prepared by either sequential dosing or by dosing from a mixture of the bulk materials.

The UHV STM used in these studies has been described previously [8]. The archetypical tripod scanner design limits the imaging speed; the scan rates used during collection of the images presented here were typically 0.4 lines per second. Image processing has been limited to low pass filtering in cases where noise was not attributed to molecular motion, and in a few cases thermal drift corrections have been made.

### 3. Results and discussion

Azulene and its isomer naphthalene represent an ideal case study to assess the ability of the STM to differentiate between structurally similar molecules. Naphthalene and azulene are both

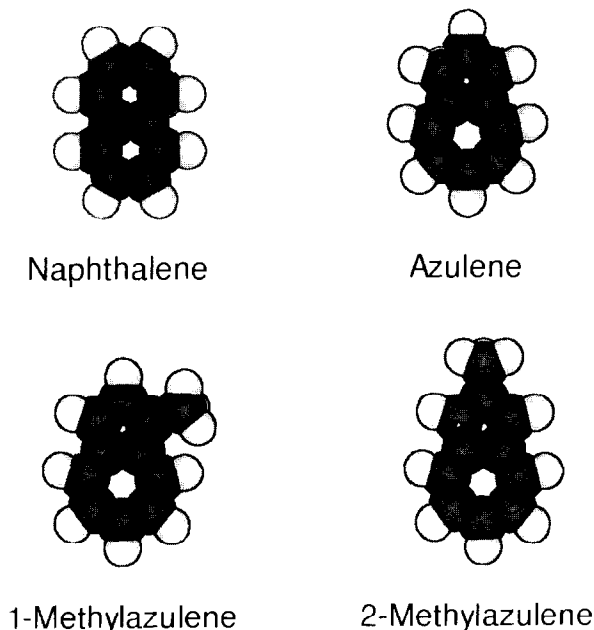


Fig. 1. Space-filling models of the four molecules studied in this work.

planar, double aromatic ring systems with the chemical formula  $\text{C}_{10}\text{H}_8$  (see fig. 1 for structures). Naphthalene, with two fused six-carbon rings, is approximately 30 kcal/mol more stable than the strained five-carbon and seven-carbon ring structure of azulene. Molecular desorption of either azulene or naphthalene from the Pt(111) surface is precluded by molecular decomposition near  $200^{\circ}\text{C}$ , as marked by hydrogen evolution and residual surface carbon [9]. Both molecules form ordered monolayer structures on Pt(111) which have been previously studied in detail, particularly by LEED [9–12], affording the opportunity to compare STM images with proposed organizational models. Although azulene possesses a significant dipole moment for a pure hydrocarbon molecule,  $\sim 0.8$  D [13], adsorption with the ring system parallel to the surface plane leads to large intermolecular spacings (three times the platinum lattice spacing of  $2.77 \text{ \AA}$ ), so that dipole–dipole interactions are expected to play little role in its two-dimensional organization. No reports of spectroscopic studies or work function change measurements to assess the effects of adsorption on azulene have been reported in the literature.

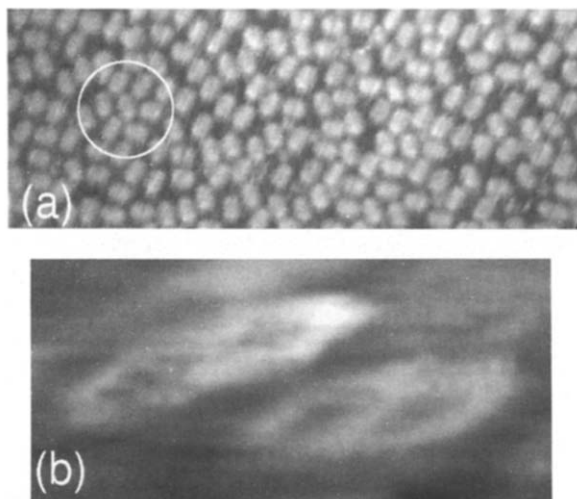


Fig. 2. (a) Typical image of ordered naphthalene on Pt(111). Image size  $\sim 90 \text{ \AA} \times 230 \text{ \AA}$ ; tip bias  $-0.16 \text{ V}$ ; tunneling current  $0.3 \text{ nA}$ . (b) A small excerpt from a high resolution image of naphthalene.  $\sim 12 \text{ \AA} \times 25 \text{ \AA}$ ;  $-0.04 \text{ V}$ ;  $1 \text{ nA}$ .

Although adsorption of substituted azulenes on Pt(111), to our knowledge, has not been previously studied, several methyl-substituted species have been included in these STM investigations. Comparison of naphthalene and azulene STM images with those of two monomethylazulene isomers yields significant insight into the effects of substituents on the STM images as well as orientation and surface mobility.

### 3.1. Pure naphthalene adsorption

Extensive results for real space imaging of naphthalene on Pt(111) have appeared elsewhere [5–7]. Although some review is necessary to facilitate comparisons with the new azulene and methylazulene data, these results will be only briefly summarized here, in order to present new discussions of naphthalene packing and high resolution imaging.

Typically, naphthalene molecules appear as elongated bi-lobed features, such as those shown in fig. 2a, with three easily identified equivalent orientations separated by rotations through  $120^\circ$ . The observed molecular spacing is consistent with  $(3 \times 3)$  spacing of the molecular centers, and detailed mappings onto such a lattice allow assign-

ment of the absolute molecular orientation with the long axis parallel to the close-packed directions of the (111) surface. The dual requirements of long axis alignment with the  $[1\bar{1}0]$  directions and three-fold symmetry of the adsorption site determine the lowest possible symmetry adsorption site to be the on-top position.

The image of fig. 2a is typical of the ordered preparation of naphthalene on Pt(111) exhibiting a distinct  $(6 \times 3)$  LEED pattern, made in this study by exposure of a warm (between 100 and  $200^\circ\text{C}$ ) substrate to naphthalene vapor. Previous LEED investigations [10–13] of this system have proposed that this adsorbate organization arises from a “herringbone” unit cell, where alternating rows of molecules have different orientation. The STM images clearly reveal the absence of any such herringbone organization, although a significant degree of order is discernable. A herringbone array would necessarily restrict the component molecules to only two of the three observed orientations, with three equivalent domains needed to account for all three allowed orientations. This type of structure is entropically unfavorable, and its absence in the STM images indicates that orientational entropy is larger than the enthalpy to be gained by organizing the molecules in such a fashion.

An alternative structure known as a pinwheel has been suggested for other adsorption systems with  $(6 \times 3)$  symmetry [14]. The pinwheel structure, where a central molecule is surrounded by six molecules with orientations systematically rotating by  $120^\circ$  in the same direction around the wheel, obviates the need for equivalent domains. Although partial pinwheels can be observed in the STM images (see the area marked in fig. 2a), close inspection shows that such rings of molecules never possess true pinwheel structure. Uniform rotation of molecules about the ring is never observed because of interactions between the central molecule and the ring molecules. Since the central molecule also possesses one of the three possible orientations, formation of a true pinwheel would require that two of the ring molecules have long axes collinear with that of the central molecule. Statistical analysis of naphthalene organization has shown that this end-on

configuration is not allowed for close-packed molecules on a  $(3 \times 3)$  superlattice. Pinwheels have been suggested when molecular interactions, such as quadrupole–quadrupole interactions, are strong enough to preferentially arrange the molecules such that a central molecule has different orientation, e.g. with the molecular long axis oriented normal to the surface [14]. Although naphthalene molecules are sometimes observed by STM with the plane of the rings not parallel to the metal surface, such tilted molecules are never present within close-packed domains, but only at domain boundaries or in disordered regions. Statistical analysis of the significant degree of order exhibited in the STM images discloses that symmetries such as glide planes required for  $(6 \times 3)$  symmetry [15] are present at  $\sim 40\%$  levels. The naphthalene/Pt(111) system thus exhibits “pseudo”- $(6 \times 3)$  symmetry consistent with the observed diffraction pattern.

While the typical appearance of naphthalene molecules is the elongated, bi-lobed structure shown in fig. 2a, higher resolution images may be acquired on rare occasions when specific, but undetermined, tip characteristics are obtained. Often, the detailed internal structure varies among the three equivalent orientations, indicating that asymmetry of the tunneling tip affects the images. fig. 2b shows an excerpt from an image where all three orientations exhibit identical internal structure, although only two orientations are shown in the magnified view. The double ring structure of naphthalene appears conclusively in images with such ultrahigh resolution, but no segmentation of the rings is noted, in contrast with previous images of benzene [1–3].

Although naphthalene is irreversibly chemisorbed onto Pt(111), the barriers to rotation and translation are surmountable at room temperature. Low coverage adsorption results in molecules uniformly distributed over the platinum surface. Aggregation does not occur at room temperature even after several days, nor can aggregation be induced by annealing at temperatures between  $100^\circ$  and  $200^\circ\text{C}$ . This lack of aggregation indicates that attractive interactions between naphthalene molecules are not responsible for the formation of ordered structures, in agree-

ment with the earlier free energy discussion. In areas where nearby neighbors do not hinder motion, individual molecules frequently undergo rotation about the molecular adsorption center by  $\pm 120^\circ$ . A less commonly observed motion is the translation of an individual molecule by one substrate lattice vector. The low barriers to lateral motion for naphthalene on Pt(111) are interesting since thermal decomposition precludes desorption, indicating the presence of a high barrier for motion normal to the metal surface.

### 3.2. Pure azulene adsorption

Azulene on Pt(111) is a much more complicated adsorption system than naphthalene on Pt(111). A variety of ordered structures [9,16] have been produced as a function of coverage and temperature, ranging from a simple  $(3 \times 3)$  structure at near monolayer coverage to a compressed  $(10 \times 10)$  structure at higher coverage, where the molecular rings must tilt out of the surface plane. Selective orientation of azulene domains depending upon substrate defects has also been reported [17]. Azulene does not form a  $(6 \times 3)$  overlayer as does its isomer naphthalene. This dissimilar behavior indicates that the interactions between azulene and the Pt(111) surface are distinctly different from those for naphthalene and Pt(111).

Exposure of the clean Pt(111) surface to azulene under conditions identical to those which produce saturated, ordered naphthalene monolayers produces an adsorbed layer of considerably less than monolayer coverage. By comparing doses required for full monolayer coverage of naphthalene and azulene, the sticking coefficient of azulene has been estimated from these STM studies to be approximately one quarter that of naphthalene. While naphthalene molecules undergo rotation and translation at submonolayer coverage, this motion is slow compared to the image acquisition time of five to ten minutes. For azulene, the situation is significantly different. The image shown in fig. 3a is typical for incomplete monolayers of azulene on Pt(111). The molecular coverage in this experiment is approximately 0.2 monolayers, much higher than indicated by the

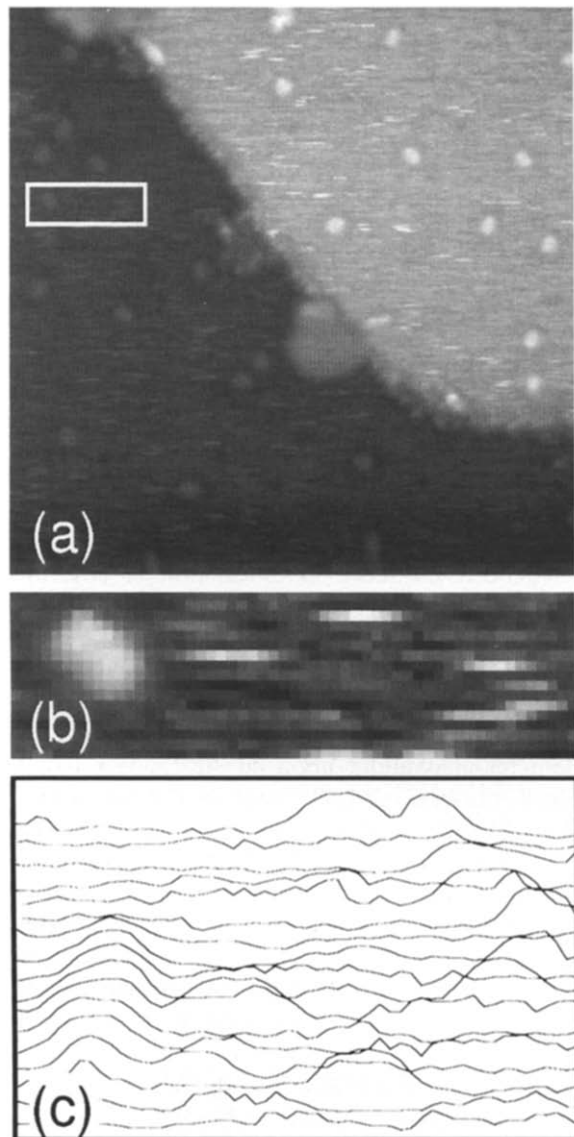


Fig. 3. (a) Low coverage azulene on Pt(111). The hexagonal feature located at the step in the center of the image is a carbon island. The resemblance of the few fixed features to naphthalene suggests they may be due to impurities from the gas handling line.  $\sim 300 \text{ \AA} \times 300 \text{ \AA}$ ;  $-0.18 \text{ V}$ ;  $0.3 \text{ nA}$ . (b) Inset marked in (a), showing one fixed molecule and single-line "dashes". (c) Line scans for (b), revealing that the dashes have the height and width expected for azulene molecules.

few fixed features. Indeed, individual STM scan traces corroborate a higher concentration. As the line scan presentation (fig. 3c) of the small marked area shows, on a given scan line more molecular

features are present than would be deduced from the top view image alone. These other molecular features do not correlate from line to line, but appear in the top view as a substantial noise component. These molecules seem to be moving at a rate comparable to the line scan speed. Tip interactions as a source of the molecular motion cannot be eliminated, but no correlations of molecular motion direction with scan direction were observed. The similar appearance of the localized features to naphthalene molecules may in fact be due to a small amount of residual naphthalene in the gas line coupled with its higher sticking coefficient.

Increasing the coverage to a full monolayer effectively hinders molecular motion and allows resolution of individual molecules (fig. 4). The molecular organization observed in such images consists of domains of close-packed molecules. The intermolecular spacings are consistent with three times the Pt lattice spacing, and no higher coverage ( $10 \times 10$ ) domains appear in any of these images at this coverage. The edges of the carbon islands [7] in the midst of the azulene overlayer provide an inherent marker of the close-packed directions on the platinum surface, since it was not possible to directly image platinum atoms simultaneously. The observed alignment of the close-packed molecular directions with the platinum lattice and the measured molecular spacing are in complete accord with the  $(3 \times 3)$  LEED pattern obtained from this sample.

Unlike naphthalene, the two rings are not even partially resolved; azulene does not appear to have any appreciable asymmetry in these room temperature images. Because such a high degree of mobility for azulene on the platinum surface has been observed, it is plausible to propose that the lack of asymmetry in the images arises from rapid rotation of azulene molecules within individual adsorption sites. Such rotational diffusion would also explain the lack of a higher level organization of azulene, such as the  $(6 \times 3)$  structure, which would require distinct orientation of the molecules with respect to the substrate lattice. The ability of azulene to accommodate higher surface coverages via tilting of the ring system out of the plane of the surface and the low sticking

coefficient is also consistent with such a weak azulene–platinum interaction. These observations are in agreement with packing calculations for azulene monolayers [18], based on van der Waals interactions, which have predicted that rotation, translation and tilting of azulene molecules should be facile. Of course, both rotational and translational motion should be eliminated by imaging at low temperature, and measurements over a range of temperatures would permit evaluation of rotational and translational diffusion constants.

Azulene coverages intermediate between 0.2 and one monolayer have also been investigated. Intermediate coverages also result in a large degree of motion, with some limited organization of azulene molecules in constricted areas, such as on narrow terraces or between carbon islands and nearby platinum steps. In this case, the azulene molecules again are circular and exhibit no asymmetry. As in the case of naphthalene, no molecular aggregation is observed, supporting the supposition made earlier that dipole–dipole interactions for adsorbed azulene are too weak to influence molecular organization.

### 3.3. Coadsorbed naphthalene and azulene

The characteristics of the tunneling tip in the imaging process dominate the effective resolution to such an extent that some method of eliminat-

ing this variation when imaging different species is desirable. Consequently, imaging two molecules in mixed monolayers serves to abolish a large number of potential effects from this source. The ability to recognize different molecules in the same image is also a general requirement for future uses of the STM to analyze surface reactions. Indeed, coadsorbed layers of naphthalene and azulene give a valuable view of the relative interactions of the two molecules with the Pt(111) surface.

Fig. 5 constitutes a pair of sequential images from a coadsorbed layer of naphthalene and azulene at a low total coverage of approximately 0.2 monolayers. This sample was prepared by dosing naphthalene and azulene simultaneously from a bulk mixture, whereby the relative concentrations of naphthalene and azulene on the surface can be estimated from vapor partial pressures at gas line temperature [19,20],  $P_{\text{naphthalene}}/P_{\text{azulene}} \approx 3.4$ , and relative sticking coefficients,  $\sigma_{\text{naphthalene}}/\sigma_{\text{azulene}} \approx 4$ , so that azulene constitutes no more than 10% of the total adsorbate coverage. In both images, a ring of six naphthalene molecules is marked by small ellipses. Note that one of the six marked naphthalene molecules (and others in both images) appears as a tri-lobed feature in fig. 5b. Image processing of these images has been limited to low pass filtering and the superposition of elliptical markers. The markers in fig. 5b were transferred with relative positions unchanged

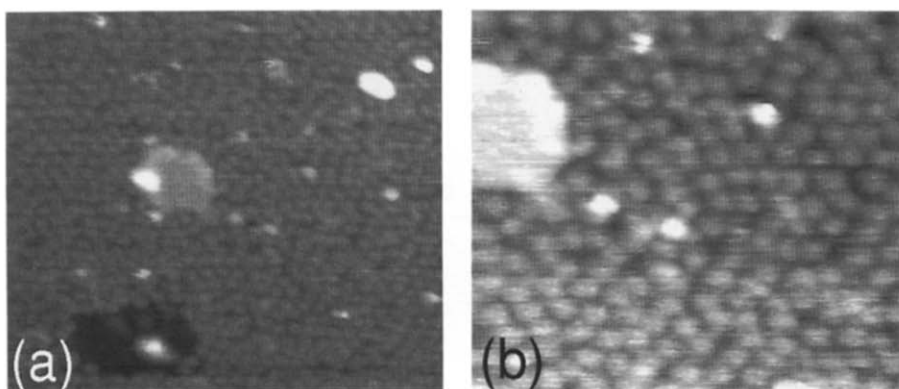


Fig. 4. (a) Saturated coverage azulene on Pt(111), showing close-packed domains with  $(3 \times 3)$  symmetry. The smooth island in the center of the image is localized carbon.  $\sim 300 \text{ \AA} \times 300 \text{ \AA}$ ;  $-1.18 \text{ V}$ ;  $0.2 \text{ nA}$ . (b) Higher resolution area from (a), confirming that the individual molecules are circular.

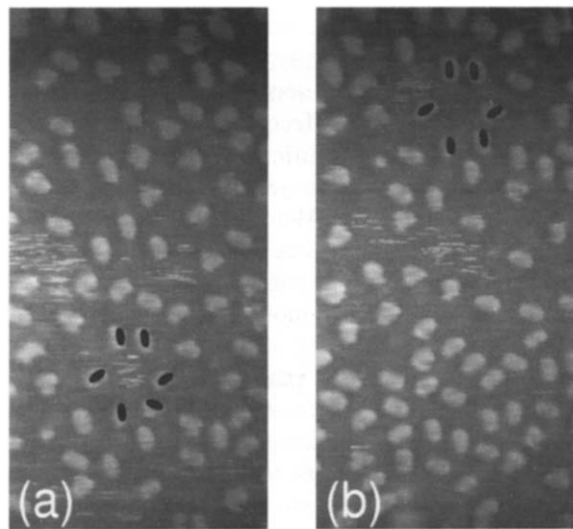


Fig. 5. Sequential images from a coadsorbed monolayer of naphthalene and azulene, with an interval of  $\sim 10$  min.  $\sim 90 \text{ \AA} \times 150 \text{ \AA}$ ;  $-0.05 \text{ V}$ ;  $0.3 \text{ nA}$ . (a) The noisy patch within the marked ring of naphthalene molecules is an azulene molecule diffusing during the scan. (b) The azulene molecule has escaped from the confining naphthalene ring.

from fig. 5a, with the exception of that for the tri-lobed naphthalene, which was rotated by  $120^\circ$  about the lower right lobe of the molecule. The tri-lobed features represent molecules which have rotated about one lobe of the molecule during the image scan. Occasional single-lobe features are also observed, where this type of rotation moves the molecule opposite to the scan direction. Such rotations about one lobe of the molecule are distinct from the more commonly observed rotations about the molecular center. Sequential rotations about one lobe of the molecule constitute one mechanism whereby the naphthalene molecules translate across the platinum surface. The noisy feature confined within the ring of marked naphthalene molecules in fig. 5a is identifiable as an azulene molecule by inspection of individual non-correlated scan lines, which are quite similar to those shown in fig. 3b. The different surface diffusion rates for naphthalene and azulene permit a graphic display of the two-dimensional cage effect [21], whereby the ring of naphthalene molecules confines the lateral motion of the azulene molecule. In Fig. 5b, the

azulene molecule has escaped from the naphthalene cage, moving to the upper left.

Near saturation coverage for these coadsorbed layers restricts mobility of the azulene molecules to a level comparable to that of complete azulene ( $3 \times 3$ ) monolayers (fig. 6). Again the azulene molecules appear circular, with no notable asymmetry. In fig. 6a, the tunneling tip provides molecular resolution but no degree of internal structure for either naphthalene or azulene. However, the naphthalene molecules are still markedly elongated, as the oval outlines show, while azulene appears more symmetric and circular. With this degree of resolution, differentiating between naphthalene and azulene is quite subtle. Higher resolution makes the distinction more pronounced. In fig. 6b, the tunneling tip can just resolve the double ring structure of naphthalene, and the presence of all three orientations indicates that molecular asymmetry is not an anomaly of the imaging process. The azulene molecules in this image are again obviously circular and are conspicuous by virtue of the presence of only a single ring.

### 3.4. Methylazulene on *Pt(111)*

Substitution at periphery positions of the azulene ring structure is expected to affect adsorption behavior. In agreement with this hypothesis, methylazulene, a mixture of 2-methylazulene and 1-methylazulene, is observed by STM to interact more strongly with the platinum surface than

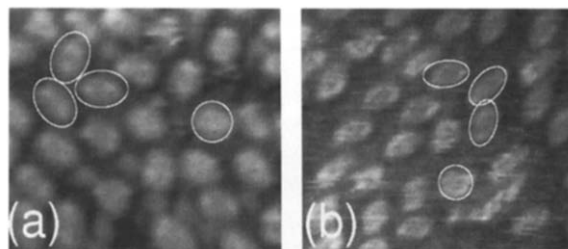


Fig. 6. Coadsorbed naphthalene and azulene with all three orientations of the elongated naphthalene molecules marked with ovals and symmetric azulene molecules marked by circles.  $\sim 90 \text{ \AA} \times 90 \text{ \AA}$ ;  $-0.05 \text{ V}$ ;  $1 \text{ nA}$ . (a) Low resolution. (b) Higher resolution, with double rings apparent for naphthalene and single rings observed for azulene.

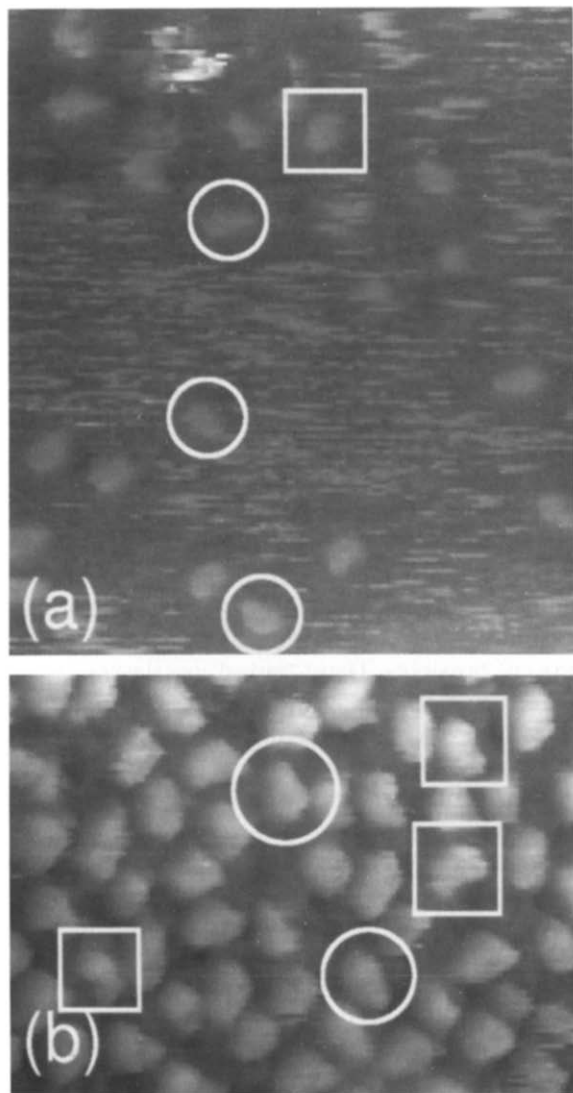


Fig. 7. (a) Low coverage methylazulene on Pt(111). The circles mark pear-shaped features associated with the 2-methylazulene isomer. The long axis is seen to be oriented in a variety of directions, and for a given orientation the asymmetry may point in either direction.  $\sim 150 \text{ \AA} \times 150 \text{ \AA}$ ;  $-0.5 \text{ V}$ ;  $2 \text{ nA}$ . (b) Near full-monolayer coverage. The squares mark different orientations of kidney-bean structures assigned to the 1-methylazulene isomer.  $\sim 120 \text{ \AA} \times 90 \text{ \AA}$ ;  $-0.5 \text{ V}$ ;  $2 \text{ nA}$ .

does unsubstituted azulene. Images of low coverage overlayers of methylazulene on Pt(111) (see fig. 7a) exhibit a higher degree of molecular localization, but again reveal that a substantial proportion of the molecules are in motion during the

scan. The circles in fig. 7a mark a few of the fixed molecules that appear to have a distinct pear-shaped asymmetry consistent with the physical structure of the 2-methylazulene isomer (see fig. 1). A number of orientations of these methylazulene molecules are observed in the low coverage images. Indeed, these 2-methylazulene molecules are similar to naphthalene in that three orientations of the long axis of the molecule are observed. These three equivalent orientations are separated by rotations through  $120^\circ$  and, for each orientation of the long molecular axis, molecules with the pear-shape asymmetry pointed in both directions are observed. Assignment of the absolute orientation requires further analysis since it has not been possible to image platinum atoms and molecules simultaneously, but the molecules clearly occupy adsorption sites with three-fold or higher symmetry.

Molecular features with an alternative asymmetry consistent with the 1-methylazulene isomer are not conspicuous in these low coverage images. There are some fixed molecules that do not exhibit the pear-shape, such as that marked by the square in fig. 7a, but the concentration of these structures is much less than that of the pear-shaped features. Since these samples were prepared by dosing from mixtures of both isomers, the lack of conspicuous 1-methylazulene isomers requires some explanation. Absence of a definitive alternative structure that can be associated with the 1-methyl isomer may be attributed to one of several possible factors. First, although the physical structures for the two isomers are quite distinct, the STM is sensitive to electronic rather than physical structure, so that similar electronic structures could appear equivalent in the STM images. Extended Hückel molecular orbital calculations, incorporating platinum atom clusters, indicate that the electronic structure for these two systems should be separable by the STM. Second, while the two molecular species were dosed simultaneously in these experiments, a large disparity in the sticking coefficients for the two isomers could reduce the relative surface concentration of 1-methylazulene compared to its isomer 2-methylazulene. Inability to assign a distinct structure to the 1-methylazulene isomer

would thus be due primarily to its scarcity in the images. Finally, different lateral mobilities on the Pt(111) surface due to substitution position could also account for the low apparent concentration of the 1-methylazulene isomer. For example, the 2-methylazulene might be localized during the image scan, as represented by the pear-shaped structures, while the 1-methylazulene is less localized due to diffusion, appearing in the mobile molecule "noise" in the low coverage images.

Saturation of the methylazulene surface coverage provides some insight to distinguish among these alternative explanations. In fig. 7b, molecular motion has been restricted to a low level by the high adsorbate coverage, although molecules can still be seen to move in areas of lower local coverage, such as the upper right portion of this image. Two distinct molecular structures are clearly present in such images. The notable pear-shape is again marked in fig. 7b by circles, and several kidney-bean shaped features consistent with the physical structure of 1-methylazulene molecules are marked by squares. The presence of several different orientations of the kidney-bean structure again eliminates tip anomalies as the origin of this asymmetry. As mentioned above, features without the pear-shaped structure were observed in the low coverage images (fig. 7a), and comparison of the two images discloses that several kidney-bean shaped molecules also appear in the low coverage image. The lower relative concentration of the 1-methylazulene is comparable in both the low and high coverage images, and can be estimated from the STM results to be about 20% of the total coverage. Assuming that the vapor pressures of the two isomers are comparable, the reduced apparent coverage of the 1-methyl isomer must be due to a significant dependence of the sticking coefficient on the substitution position of the methyl group. Quantitatively, for similar vapor pressures, the observed surface coverages imply a relative sticking coefficient of  $\sigma_{1\text{-methyl}}/\sigma_{2\text{-methyl}} \approx 0.2$ . This effect can be rationalized by considering the different asymmetry of the two isomers. The observation of tilted naphthalene molecules suggests that the initial stages of adsorption of these molecules need not require incoming molecules to have the ring sys-

tem parallel to the metal surface. However, the range of acceptable angles may be more restricted for azulene and the methylazulenes, accounting for the reduced sticking coefficients observed for these molecules. And, in the case of the two methylazulene isomers, substitution at the 1-position breaks the molecular symmetry and would reasonably narrow the range of acceptable initial adsorption geometries.

### 3.5. Coadsorbed methylazulene and naphthalene

Coadsorbed overlayers of methylazulene with naphthalene are quite useful in that such mixtures allow direct comparison of the adsorption of these molecules. The known orientations of the naphthalene molecules serve as intrinsic markers of the close-packed directions on the platinum surface, since concurrent imaging of the platinum atoms and adsorbed molecules has not proven possible. These mixed overlayers were imaged first after exposing the Pt(111) substrate to a low coverage dose of methylazulene only. Subsequent long naphthalene exposures were intended to saturate the Pt(111) surface, but since the samples were dosed at room temperature, incomplete monolayers without good adsorbate order resulted. No attempt was made to dose methylazulene and naphthalene simultaneously with the sample at room temperature, since the sticking coefficients for both methylazulene isomers are at least one order of magnitude less than that for naphthalene.

Sequential images of naphthalene/methylazulene coadsorbed overlayers consequently display some degree of molecular motion, as shown in fig. 8. Particularly notable is the motion of a 2-methylazulene molecule in the lower right portion of fig. 8, which is excessively elongated. The brighter, noisy feature in the lower central portion of fig. 8 appears to be approximately 2 Å in height, twice the typical height measured by the STM for all the molecules studied here. This height is consistent with that measured in previous naphthalene on Pt(111) experiments for molecules assigned as tilted with respect to the surface [5]. Naphthalene molecules with all three possible orientations are easily identified in such

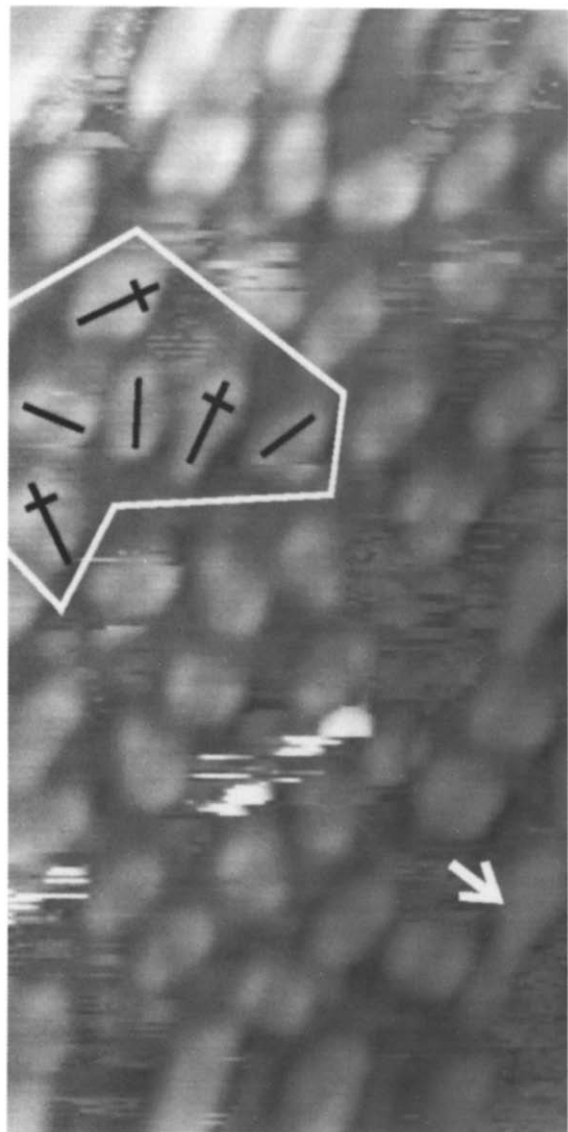


Fig. 8. Coadsorbed naphthalene and methylazulene. The arrow points to a 2-methylazulene molecule which is elongated due to movement during the image scan. The dark single lines mark examples of all three orientations of naphthalene molecules. The overall orientations for three of the six possible combinations of long axis and asymmetry orientation for 2-methylazulene are marked by dark crosses. Comparison of the molecules in the marked area easily reveals that the long axes of 2-methylazulenes are rotated by  $30^\circ$  with respect to those of the naphthalene molecules and therefore also to the close-packed direction of the underlying platinum lattice.  $\sim 90$   $\text{\AA} \times 180$   $\text{\AA}$ ;  $-0.3$  V;  $2$  nA.

images by their symmetric, bi-lobed structure. At several positions within this image, naphthalene molecules are located adjacent to 2-methylazulene molecules, making it trivial to assign the orientation of the long axis of the 2-methylazulene molecule as rotated by  $30^\circ$  with respect to that of naphthalene, and thereby with respect to the platinum close-packed directions as well.

#### 4. Conclusions

Beyond inspection of the appearance of these molecules in the STM images, it has been possible to analyze molecular organization in some detail. Repetition of perfect unit cell structures has proven unnecessary for production of monolayers that yield ordered LEED patterns, as illustrated by the observation of pseudo- $(6 \times 3)$  adsorbate organization for naphthalene on Pt(111). Attractive interactions between all four molecules studied here play no discernible role at room temperature in preferential orientation and overall adsorbate organization, although molecule-surface interactions are clearly important and very variable. While naphthalene exhibits three-fold orientation of the long molecular axis along the close-packed directions of the Pt(111) surface at room temperature, azulene appears to freely rotate even when adsorbed in a fully saturated surface layer, and 2-methylazulene orients with the long molecular axis rotated by  $30^\circ$  with respect to naphthalene and the platinum lattice.

Translational diffusion for these molecules on Pt(111) is a complex issue. Naphthalene exhibits the least translational motion at room temperature and azulene is at least two orders of magnitude more mobile, while methylazulene has an intermediate diffusion rate. The difference in diffusion rate between naphthalene and azulene is unexpected. Both molecules undergo decomposition before molecular desorption occurs [10], so that it is impossible to measure binding energies. However, simple Hückel calculations for naphthalene or azulene and a platinum cluster as a function of separation indicate that the binding energies should be comparable [22]. Of course, lateral motion depends on barriers along the sur-

face plane, which are not necessarily correlated with binding energy. The difference between various adsorption sites and orientations on the platinum surface has also been predicted by the Hückel calculations [22]. The binding energies for both naphthalene and azulene in on-top sites, whether rotated  $0^\circ$  or  $30^\circ$  with respect to the platinum near-neighbor directions, are almost identical, as are the energies for the bridge site with the axis oriented at  $0^\circ$ . But naphthalene has slightly higher calculated energies for bridge sites at  $30^\circ$  or  $90^\circ$  orientation or for a three-fold hollow site at  $0^\circ$  orientation compared with azulene. This may be indicative of lower barriers to diffusion for azulene, but more detailed energy surfaces are needed. The Hückel calculations also assumed that both molecules were adsorbed with the plane of the ring system parallel to the surface. Since packing calculations [18] indicate that barriers to tilting of the azulene ring out of the plane are small, lower diffusion barriers for the tilted molecule might alternatively account for the increased lateral diffusion. Tilting might be expected to increase the apparent height of the azulene molecules in the STM images, similar to the effect seen for tilted naphthalene molecules, but azulene and untilted naphthalene have essentially identical height, typically 1 Å.

The ability to distinguish among the four molecules investigated in this series – naphthalene, azulene, 1-methylazulene and 2-methylazulene – demonstrates the sensitivity of the STM to adsorbate structure. Not only can individual molecules be identified, but internal structure of adsorbates may be probed when appropriate tip conditions are accessible. Unfortunately, routine production of tips for ultrahigh resolution of internal molecular structure is not yet available. In particular, the capability of identifying the two methylazulene isomers, where the structural difference is simply a shift of one carbon atom for the methyl substituent position, manifests the potential utility of the STM to distinguish among similar adsorbates such as reactants and products in surface chemical reactions.

## Acknowledgements

The authors acknowledge helpful discussions with J.K. Brown, Ch. Wöll, J.C. Hemminger, T. Land and S.C. Fain.

## References

- [1] H. Ohtani, R.J. Wilson, S. Chiang and C.M. Mate, *Phys. Rev. Lett.* 60 (1988) 2398.
- [2] S. Chiang, R.J. Wilson, C.M. Mate and H. Ohtani, *J. Microsc.* 152 (1988) 567.
- [3] S. Chiang, R.J. Wilson, C.M. Mate and H. Ohtani, *Vacuum* 41 (1990) 118.
- [4] P.H. Lippel, R.J. Wilson, M.D. Miller, Ch. Wöll and S. Chiang, *Phys. Rev. Lett.* 62 (1989) 171.
- [5] V.M. Hallmark, S. Chiang, J.K. Brown and Ch. Wöll, *Phys. Rev. Lett.* 66 (1991) 48.
- [6] V.M. Hallmark, S. Chiang and Ch. Wöll, *J. Vac. Sci. Technol. B* 9 (1991) 1111.
- [7] S. Chiang, D.D. Chambliss, V.M. Hallmark, R.J. Wilson and Ch. Wöll, in: *The Structure of Surfaces III*, Eds. S.Y. Tong, M.A. Van Hove, X. Xide and K. Takayanagi (Springer, Berlin, 1991) p. 204.
- [8] S. Chiang, R.J. Wilson, Ch. Gerber and V.M. Hallmark, *J. Vac. Sci. Technol. A* 6 (1988) 386.
- [9] D. Dahlgren and J.C. Hemminger, *Surf. Sci.* 114 (1982) 459.
- [10] J.L. Gland and G.A. Somorjai, *Surf. Sci.* 38 (1973) 157.
- [11] L.E. Firment and G.A. Somorjai, *Surf. Sci.* 55 (1976) 413.
- [12] D. Dahlgren and J.C. Hemminger, *Surf. Sci.* 109 (1981) L513.
- [13] H.J. Tobler, A. Bauder and Hs.H. Günthard, *J. Mol. Spectrosc.* 18 (1965) 239.
- [14] S.C. Fain, Jr. and H. You, in: *The Structure of Surfaces: Selected Papers*, Eds. M.A. Van Hove and S.Y. Tong (Springer, Berlin, 1984) p. 413.
- [15] B.W. Holland and D.P. Woodruff, *Surf. Sci.* 36 (1973) 488.
- [16] D. Dahlgren and J.C. Hemminger, *J. Chem. Phys.* 75 (1981) 5573.
- [17] C.R. Flores and J.C. Hemminger, *Surf. Sci.* 202 (1988) 433.
- [18] A. Gavezzotti and M. Simonetta, *Chem. Phys. Lett.* 92 (1982) 16.
- [19] Naphthalene critical constants from: *Handbooks of Chemistry and Physics* (CRC Press, Cleveland, 1972).
- [20] A. Bauder and Hs.H. Günthard, *Helv. Chim. Acta* 45 (1962) 1698.
- [21] E. Rabinowitch and W.C. Wood, *Trans. Faraday Soc.* 32 (1936) 547.
- [22] A. Gavezzotti, E. Ortoleva and M. Simonetta, *Chem. Phys. Lett.* 98 (1983) 536.